EUROPEAN ORGANIZATION FOR NUCLEAR RESEARCH

CERN-PPE / 93-71
22 March 1993

MEASUREMENT OF HADRON SHOWER PUNCHTHROUGH IN IRON

RD5 Collaboration, CERN, Geneva, Switzerland

Aachen[1,†] – Amsterdam (NIKHEF-H)[2]– UCLA[3]– UC Riverside[4]–CERN[5]– Helsinki[6] – Helsinki (SEFT)[7] – Madrid (CIEMAT)[8,‡] – Nijmegen[9] – Padova[10] – Roma "La Sapienza"[11] – Roma "Tor Vergata"[12] – Turku[13] – Vienna (HEPHY)[14] – Warsaw[15,*] Collaboration

M. Aalste[7], M. Andlinger[14,5], C. Bacci[11], Gy. L. Bencze[5,a], R. Bergman[9], A. Bettini[10], A. Böhrer[1,b], R. Brenner[13], C. Brouwer[9], R. Cardarelli[12], P. Casoli[10], S. Centro[10], F. Ceradini[11], D. Chrisman[3], G. Ciapetti[11], D. Cline[3], M. Della Negra[5], A. Di Ciaccio[12], W. Dominik[13], K. Doroba[15], K. Eggert[5], H. Faissner[1], A. Ferrando[8], W. Gorn[4], M. Górski[15], A. Hentinen[6], A. Hervé[5], I. Hietanen[7], V. Karimäki[7], R. Kinnunen[6], A. Kluge[14], A. C. König[9], J. Królikowski[15], F. Lacava[9], J.G. Layter[4], S. Lazic[3], J. Lindgren[7], G. Margutti[11], R. Martinelli[10], L. Martinez-Laso[8], A. Meneguzzo[10], T. Moers[1], A. Nisati[11], K. Österberg[13], S. Otwinowski[3], E. Petrolo[11], M. Pimiä[7], H. Plothow-Besch[5], C. L. A. Pols[9], L. Pontecorvo[11], R. Priem[1], E. Radermacher[5], H. Reithler[1], C. Rönnqvist[13], L. Ropelewski[13], R. Santonico[12], R. Schleichert[1], H. Schwarthoff[1], C. Seez[5,c], B. C. Shen[4], F. Szoncso[14], R. Szwed[15], E.Torrente Lujan[8], H. Tuchscherer[1], J. Tuominiemi[6], T. Tuuva[7], H. van der Graaf[2], S. Veneziano[11], G. Vesztergombi[5,a], M. Voutilainen[7], H. Wagner[1], G. Walzel[14], T. Wijnen[9], G.A.A. Witteman[2], G. Wrochna[13], C.-E. Wulz[14], L. Zanello[11], and P. Zotto[10,d].

Abstract

The total punchthrough probability of showers produced by negatively charged pions of momenta 30, 40, 50, 75, 100, 200 and 300 GeV/c, has been measured in the RD5 experiment at CERN using a toroidal spectrometer. The range of the measurement extends to 5.3 m of equivalent iron. Our results have been obtained by two different analysis methods and are compared with the results of a previous experiment.

Submitted to Zeitschrift für Physik

a) Visitor from Central Research Inst. for Physics, KNKI, Budapest Hungary, partially supported by Hungarian grant OTKA-4089
b) Now at Universität Siegen, Germany
c) Visitor from Imperial College, London, U.K.
d) Now at Dipartimento di Fisica del Politecnico, Milano, Italy
†) Supported by Deutsches Bundesministerium für Forschung und Technologie
*) Supported by Polish grant KBN 2-0422-91-01
‡) Supported by Spanish CICYT grant AEN92-0829

1 Introduction

The anticipated operation of future hadron colliders at high luminosity, the Large Hadron Collider (LHC) at $\mathcal{L} > 10^{34}\text{cm}^{-2}\text{s}^{-1}$ and the Superconducting Super Collider (SSC) at $\mathcal{L} > 10^{33}\text{cm}^{-2}\text{s}^{-1}$, extends considerably the mass range for the discovery of Higgs and SUSY particles, additional W and Z bosons, and other new particles. Single lepton and dilepton triggers, in particular $Z \rightarrow l^+l^-$ triggers, will play a crucial role in tagging the decays of these heavy particles. At these extremely high luminosities, muons offer an advantage over electrons since the trigger decision can be made after a thick absorber where the particle flux is low. Unlike electrons, muons can be detected in the middle of a high flux of hadrons. It is therefore natural to consider a high luminosity detector optimized for muon detection.

Reliable punchthrough data are necessary for the design of muon triggers, which should allow a fast and efficient cut on the transverse momentum of the muons produced at the LHC and SSC. Monte Carlo studies of punchthrough can only be relied upon to the extent to which these simulations can be confirmed by experiment. At the first trigger level, the required rejection factors of several orders of magnitude necessitate an accurate understanding of backgrounds from hadronic punchthrough.

The RD5 collaboration at CERN [1] was formed to study topics related to muon detection at future hadron colliders. These topics include: measurement of the total punchthrough probability of hadronic showers, the angular and momentum distributions of punchthrough particles produced in an absorber with and without a magnetic field, trigger and muon momentum measurement studies, and tests of various types of large area muon detectors. The RD5 detector can be thought of as being a slice on a typical collider detector, having a silicon tracker, a calorimeter and muon measurement stations.

In this paper we present the first RD5 measurements of the total punchthrough probability of hadronic showers originating from negative pions incident on a stainless steel/gas tracking calorimeter as a function of penetration depth in equivalent iron. These measurements are from data taken in 1991. Analysis of other properties of punchthrough particles is in progress.

2 The RD5 detector

A schematic view of the RD5 detector [2], located in the CERN North Area H2 beam, is shown in figure 1. It consists of two magnets, a superconducting magnet (M1) [3] with a 3 Tesla field and an absorber magnet with a 1.5 Tesla field (M2) [4]. This setup can simulate a solenoidal detector with its return yoke or a toroidal spectrometer. Only M2 was powered in 1991.

The RD5 trigger in 1991 was based on 7 sets of scintillation counters marked S1 to S7 in figure 1. The beam is defined by a coincidence of S1 (10 x 15 cm^2) and S5 (15 x 15 cm^2). Whenever the rate is high enough - mainly with high momentum hadron beams - S4 (4 x 4 cm^2) is added to the trigger. In order to select muons, the counter S6 (70 x 100 cm^2) behind the calorimeter is also added to the coincidence. The S2 and S3 counters, foreseen as a veto to reject beam halo events, were written on tape and used in the off-line analysis. The S7 scintillator wall (1 x 2.5 m^2) was also used passively for muon identification.

The multiwire proportional chambers, referred to as U1 and U3 were used to define the incident beam. A more precise measurement of the incoming beam, simulating the precise knowledge of the beam spot in a colliding beam experiment, is done with a beam telescope consisting of 8 single-sided silicon strip detectors. Construction [5] and spatial resolution [6] of this type of detector has

been reported. The silicon strip detectors are 500 μm thick with a 25 μm strip pitch and a 50 μm readout pitch. Each detector consists of 512 strips and has an active area of 25.6 mm x 58 mm.

A stainless steel/gas tracking calorimeter (TRACAL) is installed inside M1. TRACAL consists of stainless steel plates interleaved with Honeycomb Strip Chambers (HSC)[7], which can measure tracks accurately. Each chamber has an active area of 61 x 80 cm^2, with 2.6 cm gaps between the absorbers. The HSCs are made of mylar foil with copper readout strips. The foil is folded in such a way that the folds are perpendicular to the strips. Two folded foils are put together with double-sided adhesive tape resulting in hexagonal cells. In the center of each hexagonal cell a wire is strung. The main purpose of TRACAL is to identify muon contamination in the hadron beam. In addition, it allows studies of the performance of the HSCs as muon detectors inside an absorber.

In order to facilitate its installation inside M1, TRACAL was separated into two units. Between the first 13 HSC chambers, the absorbers (stainless steel plates 80 x 100 cm^2) were 40 mm thick, thus totaling 12 times 0.25λ. Where λ is one interaction length. The next 12 gaps between the HSC chambers were filled with plates each 80 mm thick giving another 12 times 0.5λ. The total absorption power of TRACAL is thus about 9λ. In front of TRACAL a lead brick wall of about one interaction length (29 X_0) was installed simulating an electromagnetic calorimeter.

The absorber magnet (M2) is a 1.5 Tesla iron magnet constructed as a closed magnetic circuit, 1.8 to 2 m thick, made up of 200 mm thick steel plates. Two 8.75 cm slits are provided in the upstream section to insert Resistive Plate Chambers [8]. The 0.9 x 4.8 m^2 inner area enclosed by the iron circuit has been dimensioned to accept a muon measurement station.

In order to measure the trajectories of the muons in the RD5 spectrometer with high accuracy six muon drift chambers from the UA1 experiment [9] were installed, two in every measurement station. In each station the two chambers are mounted 60 cm apart to provide a good determination of the muon direction. Each muon station covers an area of 315 x 375 cm^2. The large area provides a measurement of the spatial distribution of hadronic showers even at large distances from the beam axis. Each chamber is made of crossed layers of long drift tubes, each 15 cm wide and 4.5 cm thick. The single point resolution of the muon chambers is on average 400 μm for tracks with the angular distribution of beam particles at RD5. The detection efficiency of each tube is about 99 % over the whole drift volume.

Resistive Plate Chambers (RPCs) are mounted on the muon drift chambers in Station 1 and Station 2 and inside the absorber magnet. They are used to study different muon trigger schemes and, together with the drift chambers, for muon track reconstruction. Each plane measures 2 x 2 m^2 and has 64 readout strips of 31 mm pitch. The planes are coupled in pairs providing one measurement in the horizontal projection, z, and one in the vertical projection, y. Station 1 (see Fig. 1) has four pairs of RPCs with two $y-z$ measurements before and after the muon drift chambers. There is one $y-z$ pair in each of the two slots in the iron toroid. Station 2 has two $y-z$ pairs with one measurement on either side of the drift chambers. The RPC efficiency was measured to be higher than 95 % [1].

3 Data analysis

During 1991 data were taken in three run periods with negative muon and pion beams. In both cases the beam momenta were 30, 40, 50, 75, 100, 200 and 300 GeV/c. The muon data were used to characterize the muon contamination in the pion beam and for detector calibration.

A pion punchthrough event and a muon event in the RD5 detector are shown in figures 2 and 3, respectively. In total 1.1 x 10^6 muon events and 1.5 x 10^6 pion events were recorded on tape. Furthermore, for detector calibration and background studies, a set of 3.6 x 10^4 events in the muon

beam and 2.8 x 10^5 events in the pion beam were taken with a random trigger and written on tape. The event statistics at each beam momentum setting used to measure punchthrough are presented in table 1

The pion beam used by RD5 contained from 3 to 8% of primary muons depending on the momentum. This muon contamination comes from pion decays in flight upstream of the detector. While muons penetrate the whole experimental setup, hadronic showers induced by pions typically have shorter penetration depths. The high muon contamination in downstream detectors requires one to use careful background subtraction procedures.

In the following sections two independent analysis methods used to measure punchthrough are described.

3.1 Analysis Method 1

We define the total punchthrough probability at a given depth x as the ratio of the number of events with at least one hit in the detector at the depth x over the total number of events. At small depths, for a given primary energy, the longitudinal shower development scales with the average hadronic interaction length. At large depths the penetrating particles in the shower are predominantly muons coming from pion and kaon decays in the shower. An accurate punchthrough measurement at large absorber depths requires the elimination of any muon contamination in the pion beam. The method described below measures punchthrough probabilities only at the absorber depths where RPC chambers are present, namely from 1.6 to 3.5 meters of equivalent iron.

The multiplicity of wires hit in the TRACAL calorimeter for 200 GeV/c muon and pion data is shown in figure 4. A clear muon contamination is present in the pion events. A cut on the hit wire multiplicity is suitable to eliminate most of these muons, but some could survive this cut, mainly muons accompanied by electromagnetic showers, producing a large number of hit wires in TRACAL. The multiplicity cut ranged from 30 hit wires at 30 GeV/c to 50 at 300 GeV/c.

All the events passing the hit wire multiplicity cut are then analyzed with a tracking algorithm that identifies tracks penetrating through all the RPC chambers. This algorithm recognizes clusters of hit RPC strips and calculates the coordinates of their midpoint. Each pair of clustered hits, separated by at least one slab of iron, defines a road, 3 strips wide, where other clusters are searched for. If three or more clusters are found in the road, a straight line fit is performed and a track is identified if the fit passes a χ^2 cut. The measured efficiency ϵ of the tracking algorithm is $\epsilon = 0.98 \pm 0.01$.

For each track, the angle α between the beam axis and the track direction in the non-bending plane is measured. While the angular distribution of the muon data peaks at small angles [Fig. 5a], the same distribution of penetrating tracks originating in pion showers is more widely spread around the beam axis [Fig. 5b]. The difference between the angular distributions of tracks from primary muons and tracks originating from pion events is used to remove the small residual muon contamination in the pion data. Tracks identified in pion events are tagged as primary muons if the sum of hits in the RPC chambers is compatible with a muon event (namely less than a total of 15 hit strips for the 8 RPC planes[1]) and if the angle α is $< 3\sigma_\alpha^\mu$, where σ_α^μ is the r.m.s width of the distribution of α measured with muon data [Fig. 5a]. With this cut the remaining primary muon contamination (e.g. $\sim 10^{-3}$ at 300 GeV/c) is removed. Finally, punchthrough probabilities are corrected for each individual RPC chamber efficiency and noise and for the efficiency of the applied cuts. This last efficiency has been estimated by a visual scan of the events that did not pass the applied cut and is greater than 90 % for all beam momenta. The error associated with

[1] A muon produces, on average, 1.3 hits in a RPC chamber.

it has been evaluated from the number of ambiguous events found in the scanning. The estimated systematic error takes into account the uncertainties in chamber noise, efficiency measurements and background subtraction. The biggest systematic errors are found at the largest penetration depths. For example, at 3.5 m of equivalent iron the relative systematic error is 15% at 30 GeV/c and 3% at 300 GeV/c.

3.2 Analysis Method 2

The second method uses hits in all detectors of RD5, i.e. hits in TRACAL wires, muon drift chambers, RPCs and also in the scintillating counter S7 mounted behind the beam dump (see Fig. 1), to find the actual penetration depth of each punchthrough particle (PThP). This method consists of the following steps: measurement of the penetration depth of the PThP in each event, subtraction of the primary muons present in the pion beam and subtraction of superimposed events (namely two events occurring within the same event trigger).

3.2.1 Penetration depth

There are 31 absorber depths d in the RD5 setup, each separated by single or grouped detector elements. The sequence of absorber materials and detector elements is presented schematically at the bottom of figure 1. It should be noted that the absorber material at depth 26 is the sum of the chamber walls and chamber support structures in Station 1.

Let us denote the existence of a hit in a particular detector i by h_i, where $h_i = 0$ means no hits in the i-th detector and $h_i = 1$ means at least one hit in the i-th detector. A hit in detector i is weighted appropriately, given the efficiency f_i and noise level g_i of that detector. The detector efficiencies are measured using muons from the dedicated muon runs. The detector noise levels are measured by triggering at random within the pion beam.

For each possible penetration depth d and event j, the probability P_d^j to obtain a given hit pattern is calculated:

$$P_d^j = \prod_i [\theta(d-i)h_i f_i + \theta(d-i)(1-h_i)(1-f_i) + \theta(i-d)h_i g_i + \theta(i-d)(1-h_i)(1-g_i)]$$

where d is the absorber depth, 1 to 31, and i ranges over all detector elements (see bottom of figure 1). $\theta(y)$ is a step function defined in the following way:

$$\theta(y) = 1 \text{ for } y \geq 0$$
$$\theta(y) = 0 \text{ for } y < 0$$

This analysis allows the different types of chambers present in RD5 to be treated in a consistent way. For any given event, the depth d having the highest probability P_d^j is called the range R of the PThP. This variable is used in the analysis to separate pions from the muon contamination, but not to calculate the final punchthrough probability, as it will be explained below.

For the distribution of penetration depth the average probability $\overline{P_d}$ is calculated, where

$$\overline{P_d} = \frac{1}{N} \sum_{j=1}^{N} \frac{P_d^j}{\sum_{k=1}^{31} P_k^j}$$

and N is the total number of events. The distribution of this variable reduces the weight of ambiguous events (i.e. an event with two or more depths having similar probabilities). For example,

it is possible to have the following hit pattern: 1 1 1 1 1 1 1 0 1 0 0 0 0 0 0. This pattern represents 7 hit chambers, a chamber with no hit, and then another hit chamber. The ambiguity arises if one must choose chamber number 7 or number 9 as the final hit chamber. One does not know if the hit in chamber 9 is definitely due to noise or if no hit in chamber 8 is due to an inefficiency. The penetration depth distribution weights properly all these cases thus enabling one to avoid arbitrarily choosing one penetration depth over another. Figure 6 shows the unnormalized penetration depth distributions for 100 GeV/c muons and pions. In figure 6b one sees a broad bump corresponding to pion induced hadronic showers stopping in TRACAL or inside the absorber magnet, and a peak, at penetration depth 31, containing events penetrating through the whole detector; this peak contains primary muons events, but also contains punchthrough particles from pion showers. The sharp peak at measurement point 27 occurs because the thickness of absorber materials are not uniform throughout the detector. This peak corresponds to those particles which leak out of TRACAL, thus producing a hit at point 26, but then stop in the thick iron plate at the beginning of the absorber magnet M2.

After the removal of background events due to primary muons and superimposed events, the pion penetration depth distribution [Fig. 6b] is integrated to obtain the final punchthrough probabilities.

3.2.2 Subtraction of Primary Muons

Muon events in RD5 are characterized by one clean minimum-ionizing track (see Fig. 3) penetrating the entire detector. However, there are frequently additional hits in TRACAL due to δ - ray production and other electromagnetic processes induced by the muon. This is reflected in having at least one TRACAL layer with a large hit multiplicity. In addition, there could also be random hits due to noise. In contrast, pion showers (see Fig. 2) typically have a high hit multiplicity in many TRACAL layers and a larger spread.

In order to separate the pion events from the muon contamination, an algorithm was developed which examines the array of hit TRACAL wires, and for each event, removes from the array the hits which correspond to the characteristics of a typical muon event. After this procedure, an excess of remaining hits should be characteristic of a pion shower.

The array of hit TRACAL wires, h_{ij}, is defined as follows:

$h_{ij} = 0$ means no hits in the j-th wire of TRACAL layer i

$h_{ij} = 1$ means at least one hit in the j-th wire of TRACAL layer i

The algorithm which removes hits from the TRACAL hit array consists of the following steps:

1. To account for the hits due to high-energy-loss electromagnetic processes, all hits are removed from the TRACAL layer having the highest multiplicity.

2. Accidental hits (e.g. hits due to noise) are removed from the hit array by rejecting hits in the TRACAL layer i having the largest spread, defined by $rms(i)$, where

$$rms^2(i) = \sum_j h_{ij}(j - \langle j \rangle_i)^2 \quad \text{and} \quad \langle j \rangle_i = \frac{\sum_j h_{ij} j}{\sum_j h_{ij}}.$$

The sum is over the wires (j) in the i-th layer.

3. To subtract the primary minimum-ionizing track, hits are removed from the cluster (up to 3 neighboring hits) closest to the beam line in each chamber.

From the remaining hits a variable called "activity" A is calculated as follows:

$$A = \sum_i rms^2(i)$$

where the sum is over all TRACAL layers. A is a measure of the shower spread and hit multiplicity.

The range R, as defined in section 3.2.1, vs. activity A are plotted in figure 7 for 100 GeV/c muons and pions. Most muon events have an activity $A = 0$ and the maximum range $R = 31$ and are separated from the pion events which have a larger activity and shorter range.

In figures 8 a and b, the activity distribution of all 100 GeV/c muons and pions are plotted. Most of the muon events are confined to the region near $A = 0$, however there is a long tail of muon events with high activity. It was found by visual scanning that these are muons accompanied by multiple δ - rays or an electromagnetic shower. In figure 8b, a peak at $A = 0$, assumed to be due to muon contamination, is clearly seen in addition to a broad peak at higher activity assumed to originate from pion showers. The origin of these two components becomes evident if one considers the activity distribution as a function of absorber depth.

In figures 8 c,d and e, the activity distribution of only those particles stopping before Station 1 ($R \leq 10\lambda$), between Station 1 and 2 ($10\lambda < R \leq 20\lambda$) and after Station 3 ($R > 30\lambda$) are plotted, respectively. Going from figure 8c to 8d the height of the histogram reduces considerably, reflecting the absorption of pion showers, while the peak presumably due to the muon contamination is absent. In figure 8e, the peak at $A = 0$ is present indicating that these events are indeed muons penetrating the entire detector; one also sees a further reduction in the peak due to pion showers. By making a cut at $A = 20$ one is able to effectively exclude the muon background. The number of additional pion events in the region $A < 20$ is estimated by first assuming that the shape of the distribution in 8e is similar to the shape of the distribution in 8d, therefore, the fraction of events with $A < 20$ should be the same in both cases. This correction factor is applied to determine the total number of pion events penetrating to this absorber depth. The number of muon events with activity $A > 20$ can be estimated by counting the fraction of muon events with $A > 20$ in figure 8a. This correction factor is also applied to the data.

For momenta less than 100 GeV/c, the pion beam also contained a small electron contamination. The amount of contamination was estimated from the number of particles which stopped in the 29 X_0 lead brick wall installed in front of TRACAL and was measured to be less than 0.05% at 30 GeV/c. The lead was not instrumented, therefore it was not possible to determine the exact nature of the particles stopping there. This uncertainty was included in the estimate of the total systematic error in the punchthrough probability.

3.2.3 Subtraction of Superimposed Events

The probability to have two events superimposed is estimated by considering runs with a random trigger and by visual scanning. It was found that these events are mainly halo muons parallel to the beam and almost uniformly distributed over the whole area of muon chambers (4 x 3 m^2). However, most of the superimposed tracks were not reconstructed by the muon drift chambers because of time misalignment. The misalignment occurs because drift times are measured with respect to the t_0 defined by the arrival time of the primary beam particle. The true arrival time of these superimposed particles is actually $t_0 + \delta t$. Therefore a cut on the χ^2 of these reconstructed tracks

successfully vetoes most of these particles. An additional opportunity to decrease this background is given by the RPCs. The RPCs see only a fraction of the superimposed tracks due to their short gate time (70 ns). Requiring hits in both muon drift chambers and RPCs further reduces this background.

Events having at least one reconstructed track in Station 2 or Station 3 and an activity in TRACAL greater than 2 (to suppress pure muon events) were selected for visual scanning. The superimposed events were identified by having, in addition to a hadronic shower in TRACAL, a clearly visible straight track through the muon detectors parallel to the beam, but off the beam position. The results of the visual scanning are presented in table 2. It was found that at 30 GeV/c, 75% of all events reaching Station 3 ($R > 30\lambda$) were superimposed events. This fraction decreases to 37% at 300 GeV/c. These events were rejected from the data sample. The estimated error of this background subtraction was determined by the number of events which were candidates for superimposed events, but could not be clearly identified. This error is included into the total systematic error of the punchthrough probability.

4 Results

The results of methods 1 and 2 are presented in figure 9 and tables 3 and 4. Figure 9 shows the total punchthrough probability vs. meters of equivalent iron for 30, 40, 50, 75, 100, 200, and 300 GeV/c incident pions. These curves are characterized by two distinct regions, a hadronic component and a tail composed mainly of penetrating decay muons. The punchthrough probability was measured up to a depth of 5.3 m of equivalent iron. The large systematic error is dominated by the subtraction of superimposed events. In order to reduce this background, a large area veto system which covers the acceptance of the muon chambers is being installed for the 1992 runs.

In figure 9, the RD5 results have been compared with the measurements of the CCFR experiment [10] [11]. For depths <1.7 m of equivalent iron the RD5 measurements are lower than those of the CCFR. The first factor which could account for this discrepancy is the different acceptance of the two detectors. The RD5 calorimeter, TRACAL, has an active area 61 x 80 cm^2 while the CCFR calorimeter module is 300 x 300 cm^2, thus some shower particles in TRACAL produced at large angles are undetected. Secondly, the punchthrough measurement depends on the sensitive material of which the calorimeter is constructed. For example, the CCFR calorimeter, which is composed of iron plates and liquid scintillator, is more sensitive to the neutron component of the hadronic shower than TRACAL, which is a gas sampling calorimeter. The variable response to punchthrough between gas ionization detectors and scintillation counters has been reported elsewhere [11] [12].

5 Conclusions

The results of the two analysis methods used to measure punchthrough are in good agreement, indicating that neither method introduces substantial bias to the punchthrough probability as a result of its respective μ/π separation procedure. There were no RPC chambers in Station 3 during the 1991 runs, therefore a comparison between the two analysis methods was not possible at that absorber depth.

Acknowledgements

We wish to express our thanks to J. L. Benichou, D. Peach, P. Petiot and G. Waurick for their indefatigable work in the design and construction of the RD5 experiment. The continuous help of B. Powell is gratefully acknowledged. We would also like to thank the machine staff of the SPS

North Area for their expertise and help in the setting up of the H2 beam. And finally, thank you Mrs. C. Rigoni for drawing the figures.

References

[1] M. Della Negra et al., Study of Muon Triggers and Momentum Reconstruction in a Strong Magnetic Field for a Muon Detector at LHC, **CERN/DRDC/90-36, DRDC/P7.**

[2] A. Böhrer et al., Status Report of the RD5 Experiment, **CERN/DRDC/91-53.**

[3] M. Aguilar-Benitez et al., Nucl. Instr. and Meth. in Phys. Res. **A 258** (1987) 26.

[4] J.L. Bénichou, A. Hervé, G. Waurick, RD5 Technical Note **RD5-TN 91/01**

[5] I. Hietanen et al., Nucl. Instr. and Meth. in Phys. Res. **A 310** (1991) 671.

[6] I. Hietanen et al., Nucl. Instr. and Meth. in Phys. Res. **A 310** (1991) 677.

[7] H.Van der Graaf, Nucl. Instr. and Meth. in Phys. Res. **A 307** (1991) 220.

[8] R.Santonico and R.Cardarelli, Nucl. Instr. and Meth. in Phys. Res. **A 187** (1981) 377.
R.Cardarelli et al., Nucl. Instr. and Meth. in Phys. Res. **A 263** (1988) 20.

[9] K.Eggert et al., Nucl. Instr. and Meth. **176** (1980) 217.
C.Albajar et al., Z.Phys. **C44** (1989) 15.

[10] F. S. Merritt et al., Nucl. Instr. and Meth. in Phys. Res. **A 245** (1986) 27.

[11] P. H. Sandler et al., Phys. Rev. **D 42** (1990) 759.

[12] H. Fesefeldt et al., Nucl, Instr. and Meth. in Phys. Res. **A 292** (1990) 279.

Figure Captions

Fig. 1. Schematic view of the RD5 detector in its 1991 configuration.

Fig. 2. Pion event in RD5.

Fig. 3. Muon event in RD5.

Fig. 4. Multiplicity of wires hit in TRACAL for a) 200 GeV/c muons and b) 200 GeV/c pions.

Fig. 5. Angular distribution of a) 200 GeV/c muons and b) particles originating from 200 GeV/c pion showers in TRACAL.

Fig. 6 Penetration depth distribution of a) 100 GeV/c muons and b) 100 GeV/c pions. The depth scale used is the sequence of absorber materials in RD5 and is presented schematically at the bottom of figure 1. Note that the amount of absorber material is not the same in all layers.

Fig. 7 The distribution of range R and activity A of a) 100 GeV/c muons and b) 100 GeV/c pions. The vertical dotted lines indicate the range in interaction lengths λ.

Fig. 8. The activity distribution of a) 100 GeV/c muons, b) 100 GeV/c pions, c) only those pions stopping before Station 1 ($R \leq 10\lambda$), d) between Station 1 and 2 ($10\lambda < R \leq 20\lambda$) and e) after Station 3 ($R > 30\lambda$).

Fig. 9 The total punchthrough probability, as a function of meters of equivalent iron, of showers produced by negatively charged pions of momenta 30, 40, 50, 75, 100, 200 and 300 GeV/c. The results of analysis methods 1 and 2 are compared with the punchthrough measurements of the CCFR collaboration. It should be noted that the RD5 30 GeV/c data are compared with CCFR 25 GeV/c data and RD5 75 GeV/c data are compared with CCFR 70 GeV/c data. All other comparisons are made with data of the same momentum.

Table 1: Event statistics used to measure the punchthrough probability of negative pions as a function of absorber depth.

Beam Momentum [GeV/c]	Event Statistics	
	π^-	μ^-
30	84000	22000
40	82000	39000
50	40000	43000
75	52000	27000
100	75000	47000
200	63000	38000
300	42000	20000

Table 2: The fraction of all events reaching Station 3 ($R > 30\lambda$) which were identified as superimposed events.

Beam Momentum [GeV/c]	Fraction of Superimposed Events
30	0.75 ± 0.18
40	0.66 ± 0.26
50	0.67 ± 0.28
75	0.72 ± 0.22
100	0.62 ± 0.12
200	0.58 ± 0.12
300	0.37 ± 0.11

Table 3: Total punchthrough probability of 30, 40, 50, and 75 GeV/c negative pions.

m Fe eq.	30 GeV/c	40 GeV/c	50 GeV/c	75 GeV/c
0.15	0.99970 ± 0.00006	0.99984 ± 0.00005	0.99988 ± 0.00006	1.0000 ± 0.0003
0.19	0.9949 ± 0.0003	0.9965 ± 0.0002	0.9964 ± 0.0003	0.9976 ± 0.0003
0.23	0.9901 ± 0.0003	0.9928 ± 0.0003	0.9914 ± 0.0005	0.9928 ± 0.0003
0.27	0.9855 ± 0.0004	0.9897 ± 0.0004	0.9876 ± 0.0006	0.9882 ± 0.0005
0.31	0.9809 ± 0.0005	0.9867 ± 0.0004	0.9844 ± 0.0006	0.9854 ± 0.0005
0.35	0.9756 ± 0.0005	0.9839 ± 0.0004	0.9820 ± 0.0007	0.9838 ± 0.0006
0.39	0.9668 ± 0.0006	0.9793 ± 0.0005	0.9793 ± 0.0007	0.9821 ± 0.0006
0.43	0.9521 ± 0.0007	0.9718 ± 0.0006	0.9750 ± 0.0008	0.9801 ± 0.0006
0.47	0.9328 ± 0.0009	0.9611 ± 0.0007	0.9687 ± 0.0009	0.9773 ± 0.0007
0.51	0.909 ± 0.001	0.9478 ± 0.0008	0.9604 ± 0.0010	0.9740 ± 0.0007
0.55	0.883 ± 0.001	0.9309 ± 0.0009	0.950 ± 0.001	0.9696 ± 0.0008
0.59	0.845 ± 0.001	0.905 ± 0.001	0.932 ± 0.001	0.9622 ± 0.0008
0.63	0.794 ± 0.001	0.869 ± 0.001	0.905 ± 0.001	0.9501 ± 0.0009
0.71	0.713 ± 0.002	0.801 ± 0.001	0.853 ± 0.002	0.919 ± 0.001
0.78	0.617 ± 0.002	0.716 ± 0.002	0.778 ± 0.002	0.871 ± 0.001
0.86	0.520 ± 0.002	0.621 ± 0.002	0.694 ± 0.002	0.810 ± 0.002
0.95	0.437 ± 0.002	0.540 ± 0.002	0.613 ± 0.003	0.741 ± 0.002
1.03	0.357 ± 0.002	0.455 ± 0.002	0.525 ± 0.003	0.660 ± 0.002
1.11	0.286 ± 0.002	0.369 ± 0.002	0.441 ± 0.003	0.577 ± 0.002
1.19	0.226 ± 0.001	0.298 ± 0.002	0.366 ± 0.002	0.493 ± 0.002
1.27	0.175 ± 0.001	0.237 ± 0.002	0.296 ± 0.002	0.414 ± 0.002
1.35	0.137 ± 0.001	0.189 ± 0.001	0.239 ± 0.002	0.344 ± 0.002
1.43	0.106 ± 0.001	0.149 ± 0.001	0.190 ± 0.002	0.282 ± 0.002
1.51	0.0800 ± 0.0010	0.115 ± 0.001	0.148 ± 0.002	0.225 ± 0.002
1.59	0.0538 ± 0.0008	0.079 ± 0.001	0.103 ± 0.002	0.161 ± 0.002
1.69	0.0361 ± 0.0007	0.0537 ± 0.0009	0.072 ± 0.002	0.115 ± 0.002
2.29	0.0080 ± 0.0004	0.0115 ± 0.0006	0.016 ± 0.0009	0.028 ± 0.002
2.89	0.0030 ± 0.0003	0.0035 ± 0.0005	0.0046 ± 0.0007	0.008 ± 0.001
3.49	0.0018 ± 0.0003	0.0020 ± 0.0005	0.0022 ± 0.0006	0.003 ± 0.001
5.29	0.0003 ± 0.0003	0.0006 ± 0.0005	0.0007 ± 0.0006	0.001 ± 0.001

Table 4: Total punchthrough probability of 100, 200, and 300 GeV/c negative pions.

m Fe eq.	100 GeV/c	200 GeV/c	300 GeV/c
0.15	1.000000 ± 0.000003	1.000000 ± 0.000003	1.00000 ± 0.00001
0.19	0.99989 ± 0.00004	0.99993 ± 0.00003	0.99997 ± 0.00003
0.23	0.99966 ± 0.00007	0.99986 ± 0.00005	0.99995 ± 0.00004
0.27	0.99937 ± 0.00010	0.99972 ± 0.00007	0.99976 ± 0.00008
0.31	0.9990 ± 0.0001	0.99952 ± 0.00009	0.99965 ± 0.00009
0.35	0.9985 ± 0.0001	0.9993 ± 0.0001	0.9995 ± 0.0001
0.39	0.9978 ± 0.0002	0.9991 ± 0.0001	0.9993 ± 0.0001
0.43	0.9970 ± 0.0002	0.9987 ± 0.0001	0.9993 ± 0.0001
0.47	0.9959 ± 0.0002	0.9983 ± 0.0002	0.9990 ± 0.0002
0.51	0.9944 ± 0.0003	0.9979 ± 0.0002	0.9987 ± 0.0002
0.55	0.9922 ± 0.0003	0.9973 ± 0.0002	0.9983 ± 0.0002
0.59	0.9886 ± 0.0004	0.9966 ± 0.0002	0.9977 ± 0.0002
0.63	0.9823 ± 0.0005	0.9954 ± 0.0003	0.9970 ± 0.0003
0.71	0.9657 ± 0.0007	0.9920 ± 0.0004	0.9954 ± 0.0003
0.78	0.9366 ± 0.0009	0.9855 ± 0.0005	0.9927 ± 0.0004
0.86	0.892 ± 0.001	0.9736 ± 0.0007	0.9874 ± 0.0006
0.95	0.838 ± 0.001	0.9559 ± 0.0008	0.9791 ± 0.0007
1.03	0.768 ± 0.002	0.925 ± 0.001	0.9623 ± 0.0010
1.11	0.692 ± 0.002	0.883 ± 0.001	0.941 ± 0.001
1.19	0.610 ± 0.002	0.827 ± 0.002	0.907 ± 0.001
1.27	0.525 ± 0.002	0.757 ± 0.002	0.858 ± 0.002
1.35	0.448 ± 0.002	0.683 ± 0.002	0.800 ± 0.002
1.43	0.375 ± 0.002	0.603 ± 0.002	0.732 ± 0.002
1.51	0.301 ± 0.002	0.514 ± 0.002	0.650 ± 0.002
1.59	0.227 ± 0.002	0.411 ± 0.002	0.540 ± 0.003
1.69	0.167 ± 0.002	0.318 ± 0.002	0.438 ± 0.003
2.29	0.0406 ± 0.0010	0.092 ± 0.001	0.142 ± 0.002
2.89	0.0179 ± 0.0008	0.023 ± 0.001	0.036 ± 0.001
3.49	0.0043 ± 0.0007	0.008 ± 0.001	0.0114 ± 0.0009
5.29	0.0018 ± 0.0007	0.003 ± 0.001	0.0038 ± 0.0008

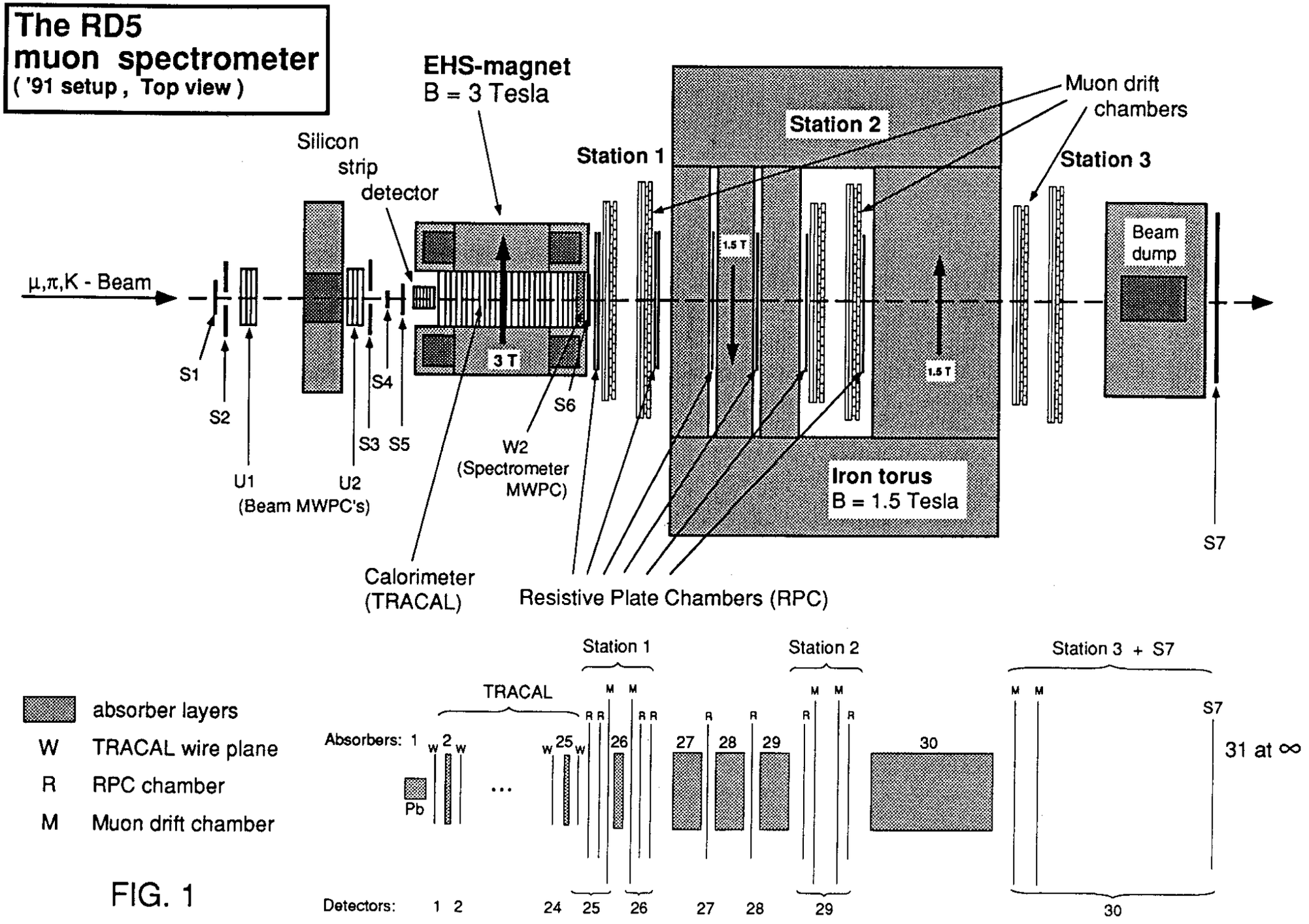
The RD5
muon spectrometer
('91 setup , Top view)
EHS-magnet
B = 3 Tesla
Silicon
strip
detector
Station 1
Station 2
Station 3
Muon drift
chambers
μ,π,K - Beam
S1
S2
U1
(Beam MWPC's)
U2
S3
S4
S5
S6
3 T
W2
(Spectrometer
MWPC)
1.5 T
1.5 T
Beam
dump
Iron torus
B = 1.5 Tesla
S7
Calorimeter
(TRACAL)
Resistive Plate Chambers (RPC)
absorber layers
W TRACAL wire plane
R RPC chamber
M Muon drift chamber
Station 1
Station 2
Station 3 + S7
TRACAL
Absorbers: 1
Pb
30
S7
31 at ∞
Detectors: 1 2 24 25 26 27 28 29 30

FIG. 1

300 GeV/c π^-

Run : 714

Event : 4172

Date : 30/08/91

Time : 14:04

M2 : 1000A

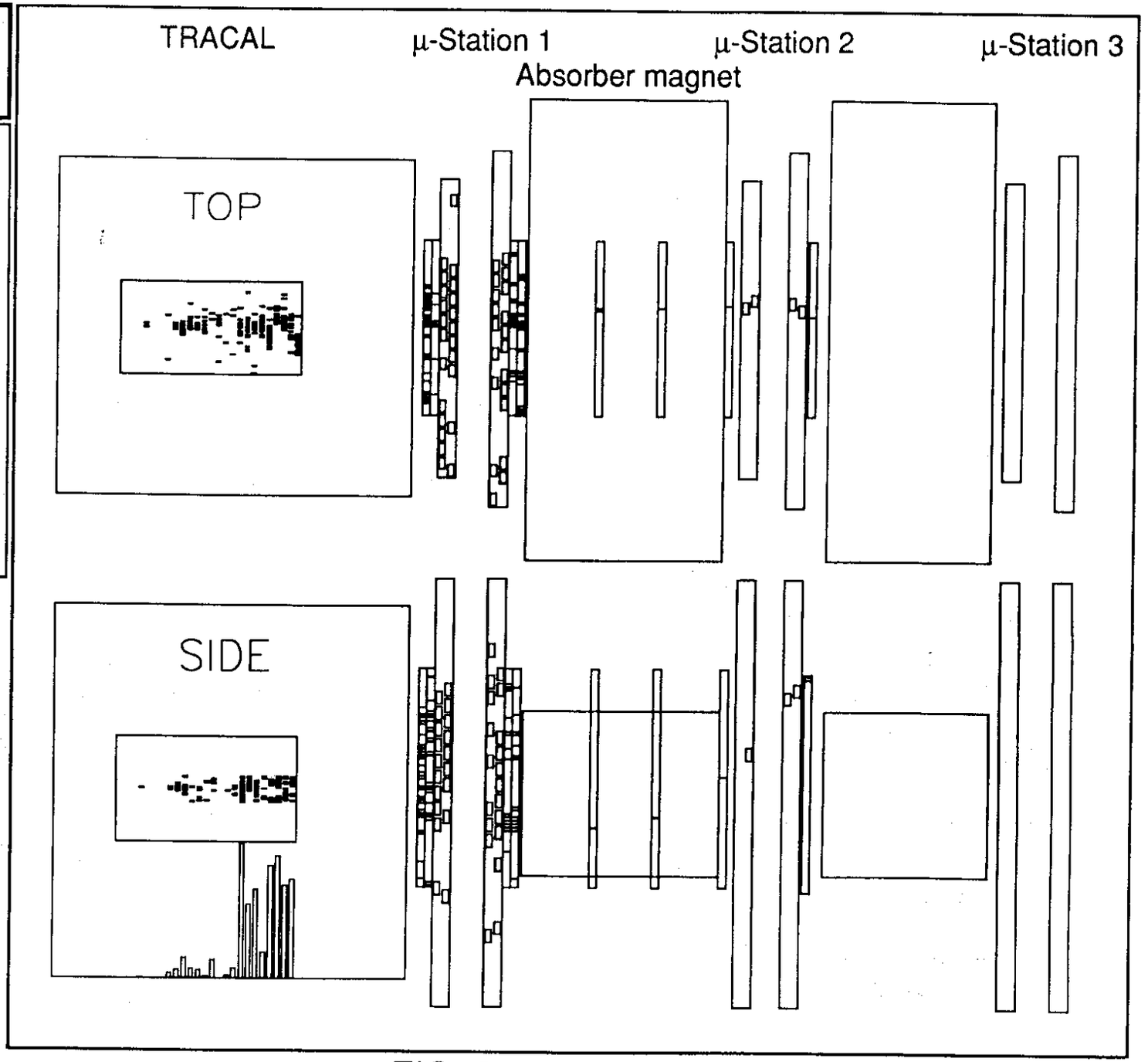

FIG. 2

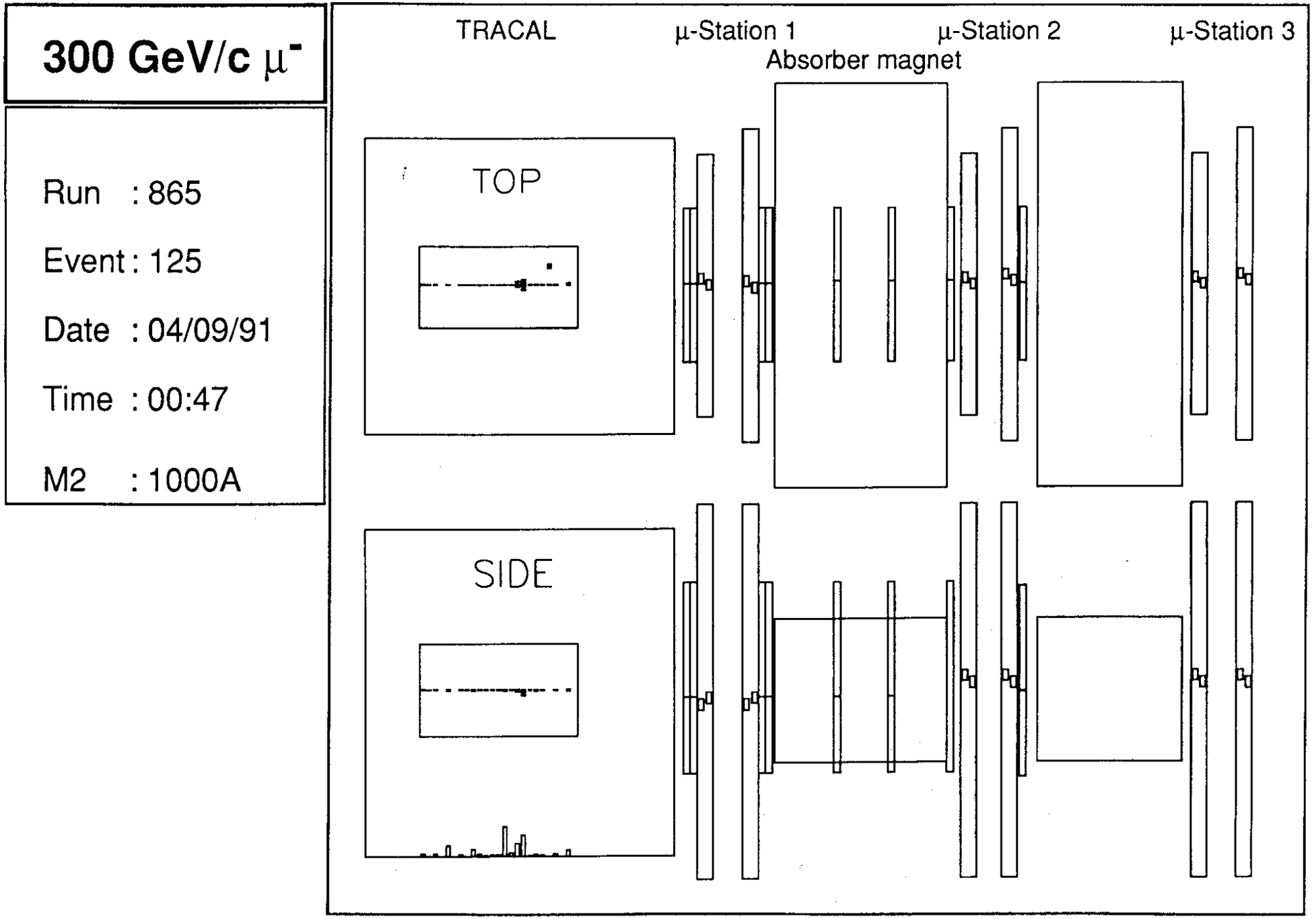
300 GeV/c μ⁻
Run : 865
Event : 125
Date : 04/09/91
Time : 00:47
M2 : 1000A
TRACAL
μ-Station 1
μ-Station 2
μ-Station 3
Absorber magnet
TOP
SIDE

FIG. 3

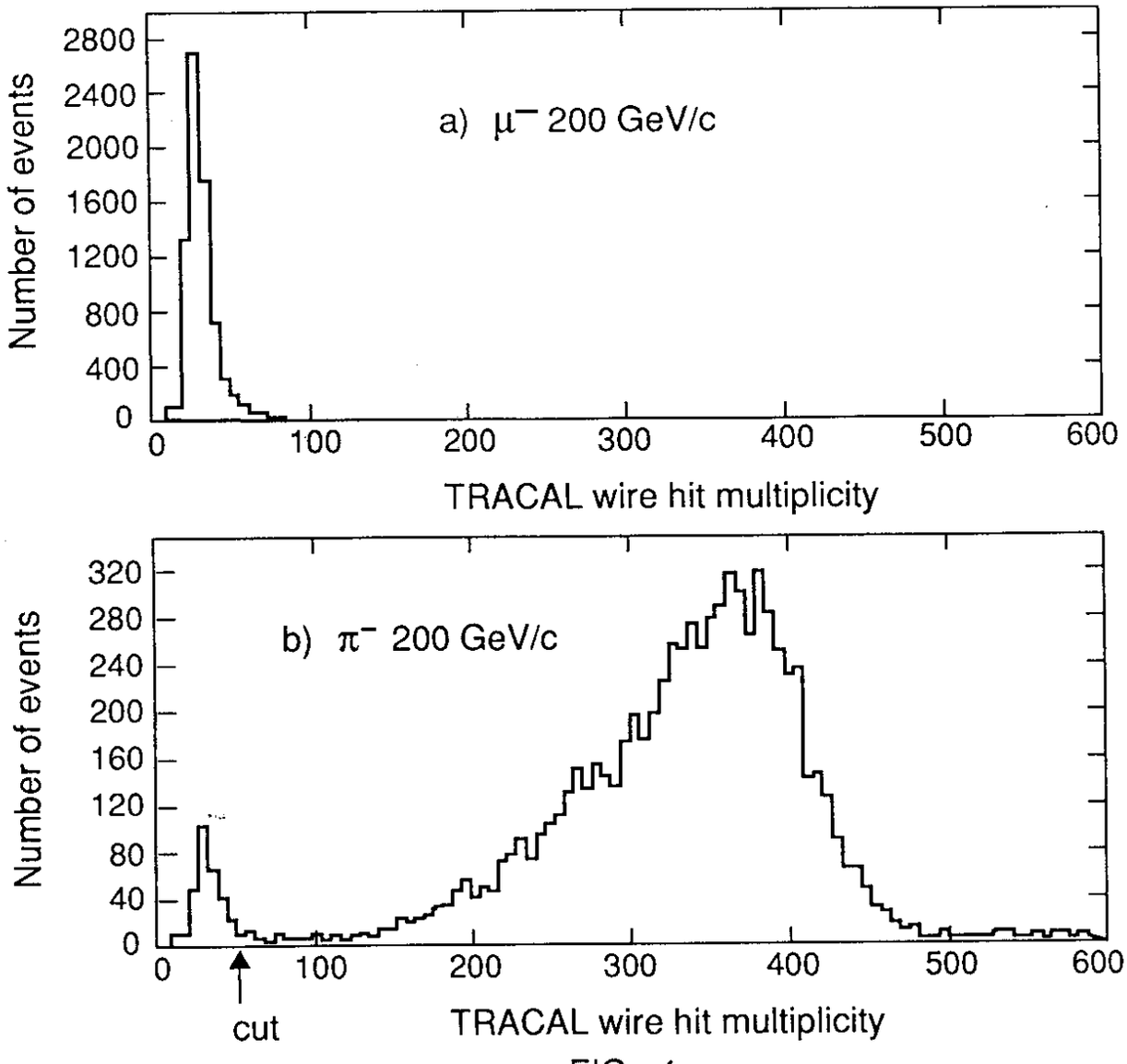
a) μ⁻ 200 GeV/c
Number of events
2800
2400
2000
1600
1200
800
400
0
0
100
200
300
400
500
600
TRACAL wire hit multiplicity
b) π⁻ 200 GeV/c
Number of events
320
280
240
200
160
120
80
40
0
0
100
200
300
400
500
600
cut
TRACAL wire hit multiplicity

FIG. 4

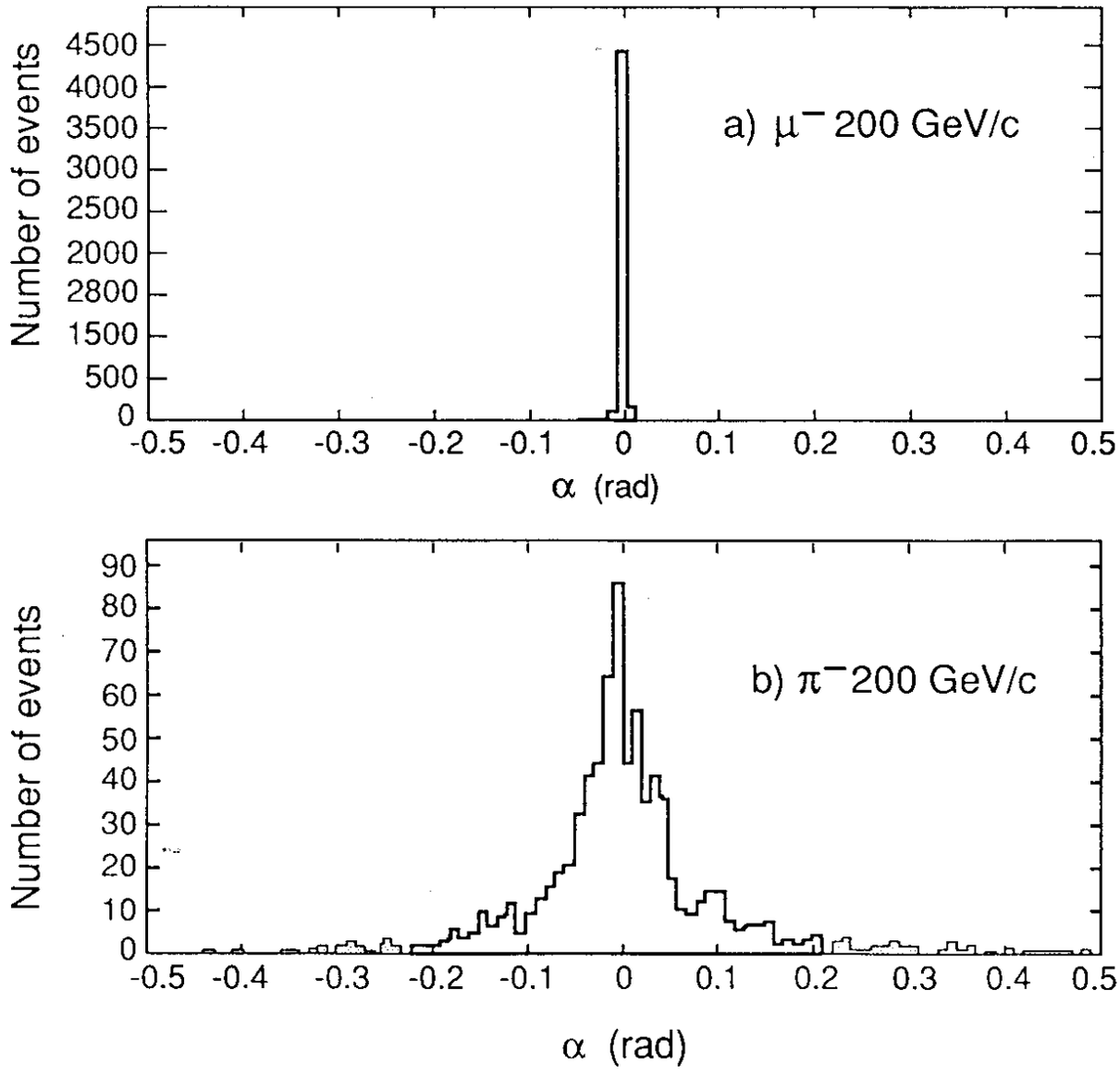
Number of events
4500
4000
3500
3000
2500
2000
2800
1500
500
0
-0.5 -0.4 -0.3 -0.2 -0.1 0 0.1 0.2 0.3 0.4 0.5
α (rad)
a) μ⁻ 200 GeV/c
Number of events
90
80
70
60
50
40
30
20
10
0
-0.5 -0.4 -0.3 -0.2 -0.1 0 0.1 0.2 0.3 0.4 0.5
α (rad)
b) π⁻ 200 GeV/c

FIG. 5

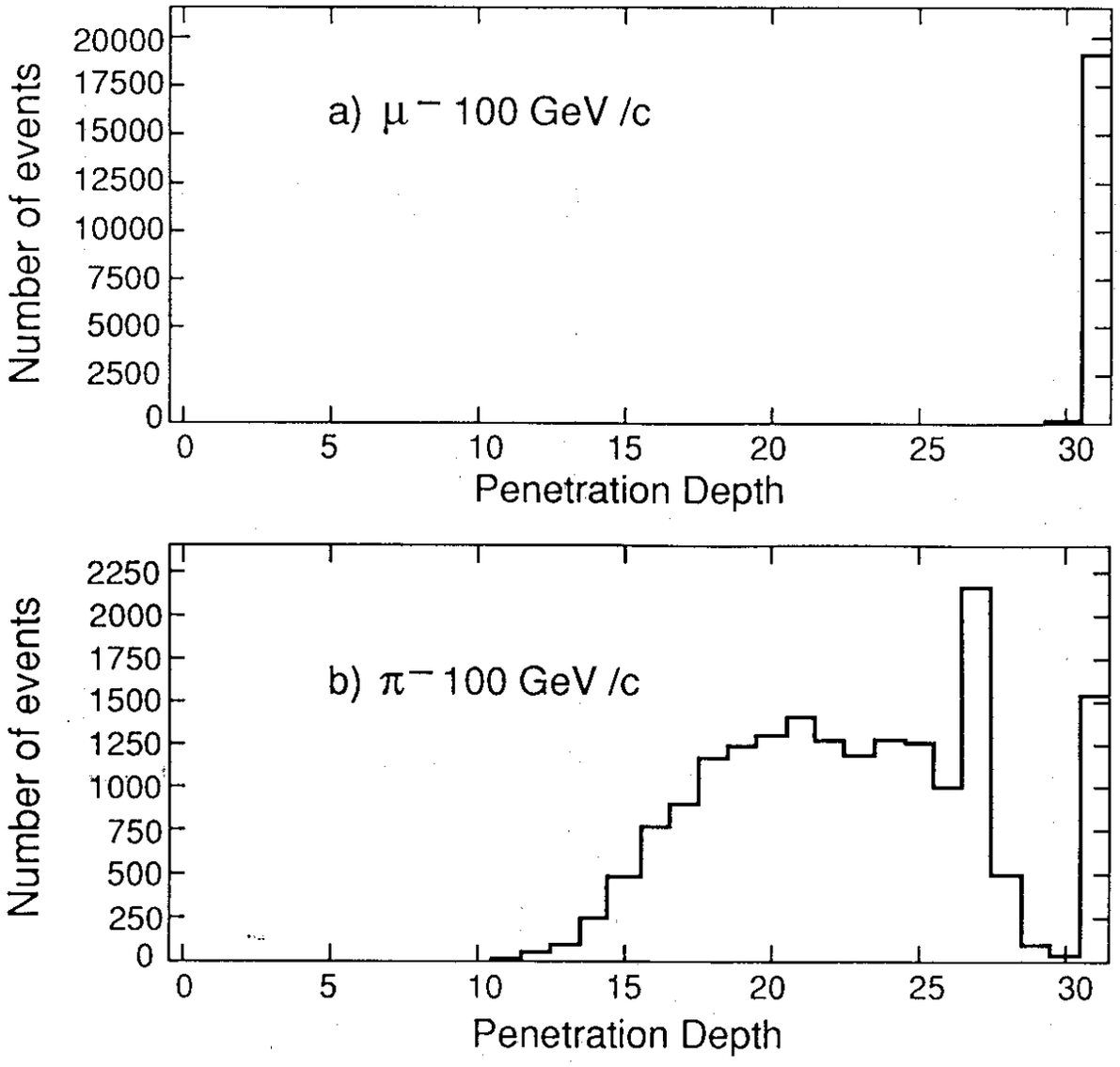
a) μ⁻ 100 GeV /c
Number of events
Penetration Depth
b) π⁻ 100 GeV /c
Number of events
Penetration Depth

FIG. 6

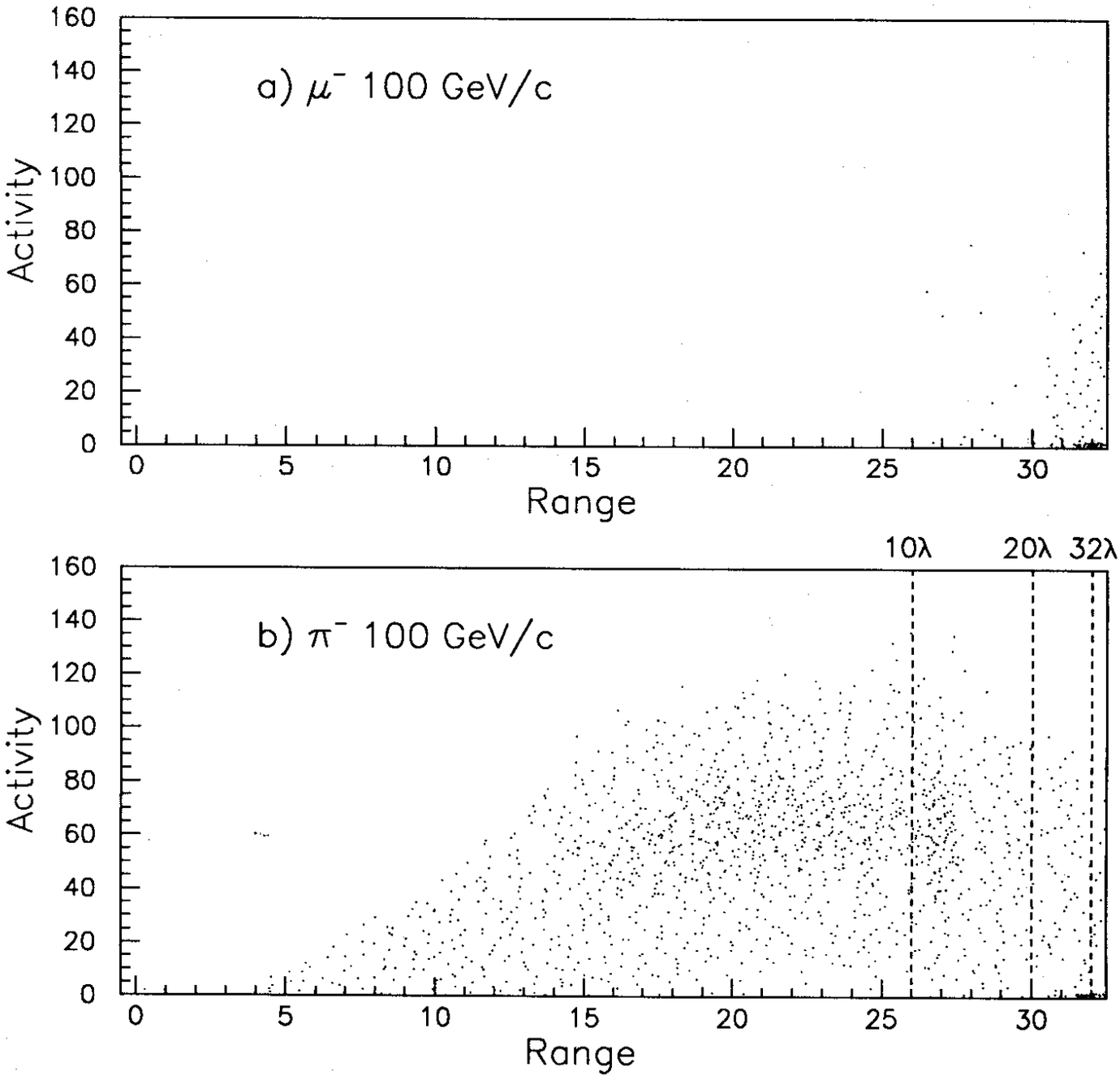
a) μ^- 100 GeV/c
Activity
Range
0
20
40
60
80
100
120
140
160
0
5
10
15
20
25
30
b) π^- 100 GeV/c
10λ
20λ
32λ
Activity
Range

FIG. 7

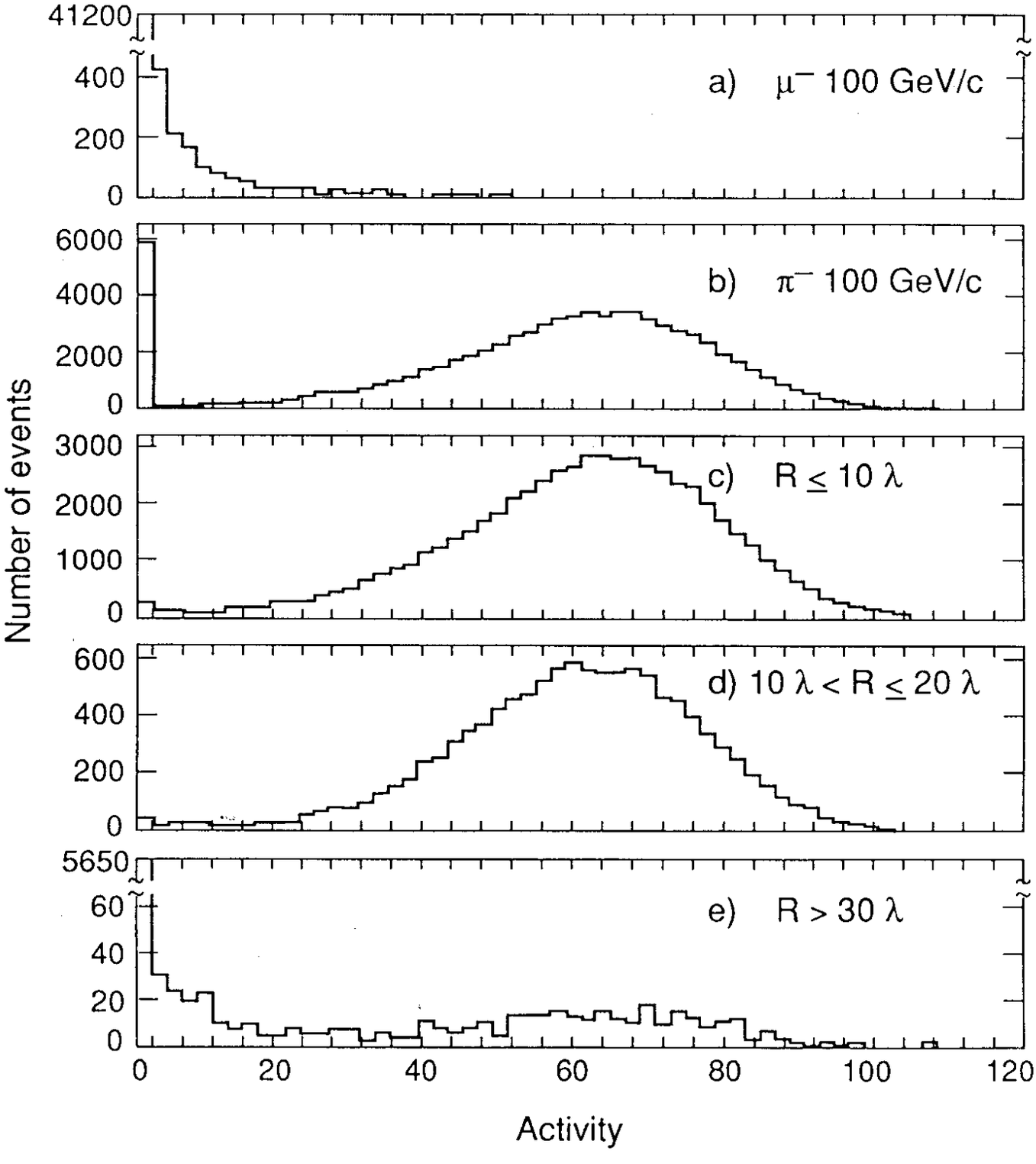
41200
400
200
0
a) μ⁻ 100 GeV/c
6000
4000
2000
0
b) π⁻ 100 GeV/c
3000
2000
1000
0
c) R ≤ 10 λ
600
400
200
0
d) 10 λ < R ≤ 20 λ
5650
60
40
20
0
e) R > 30 λ
Number of events
0
20
40
60
80
100
120
Activity

FIG. 8

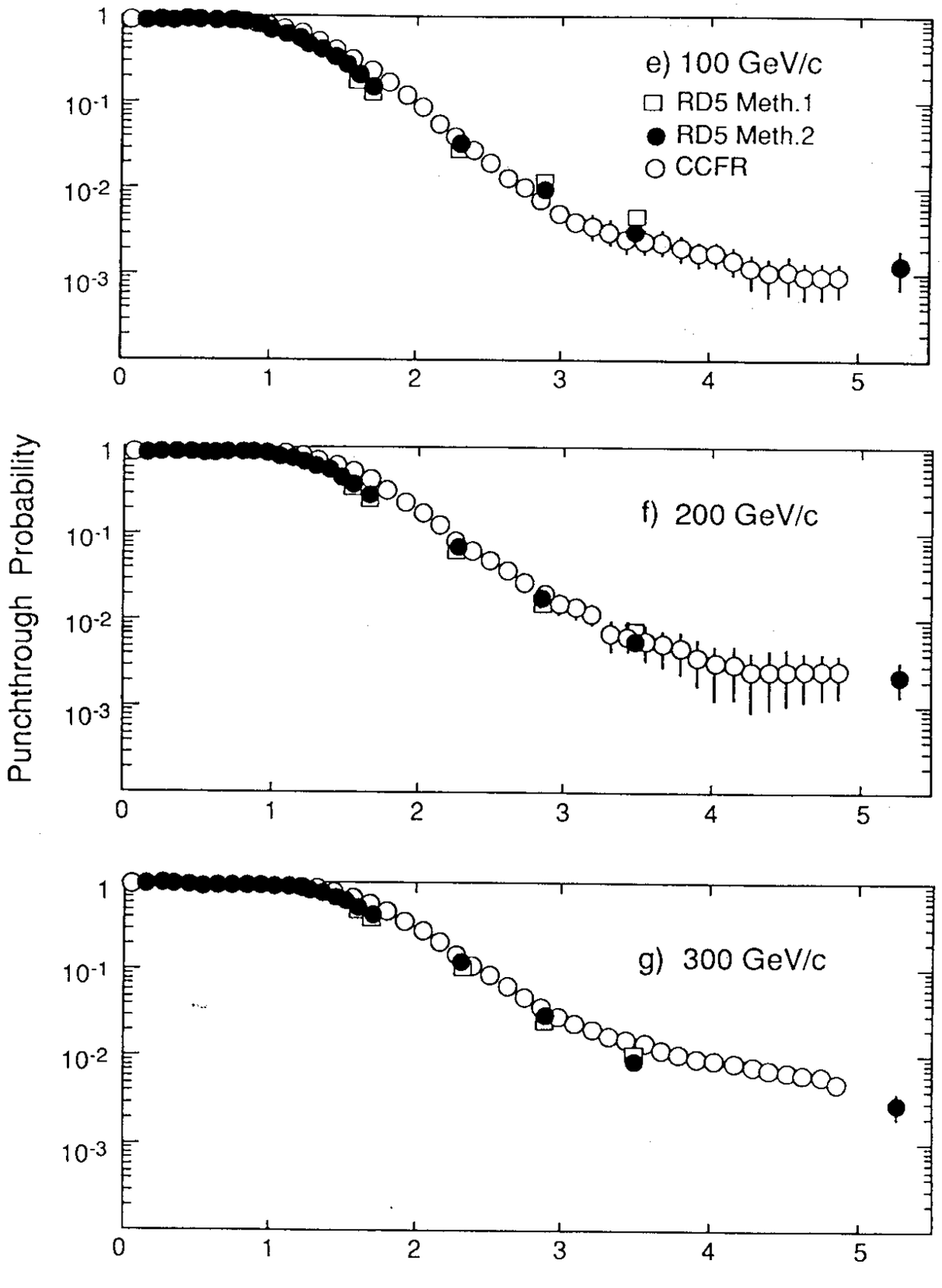
e) 100 GeV/c
RD5 Meth.1
RD5 Meth.2
CCFR
f) 200 GeV/c
g) 300 GeV/c
Punchthrough Probability
m Fe Equivalent
1
10-1
10-2
10-3
0
1
2
3
4
5

FIG. 9

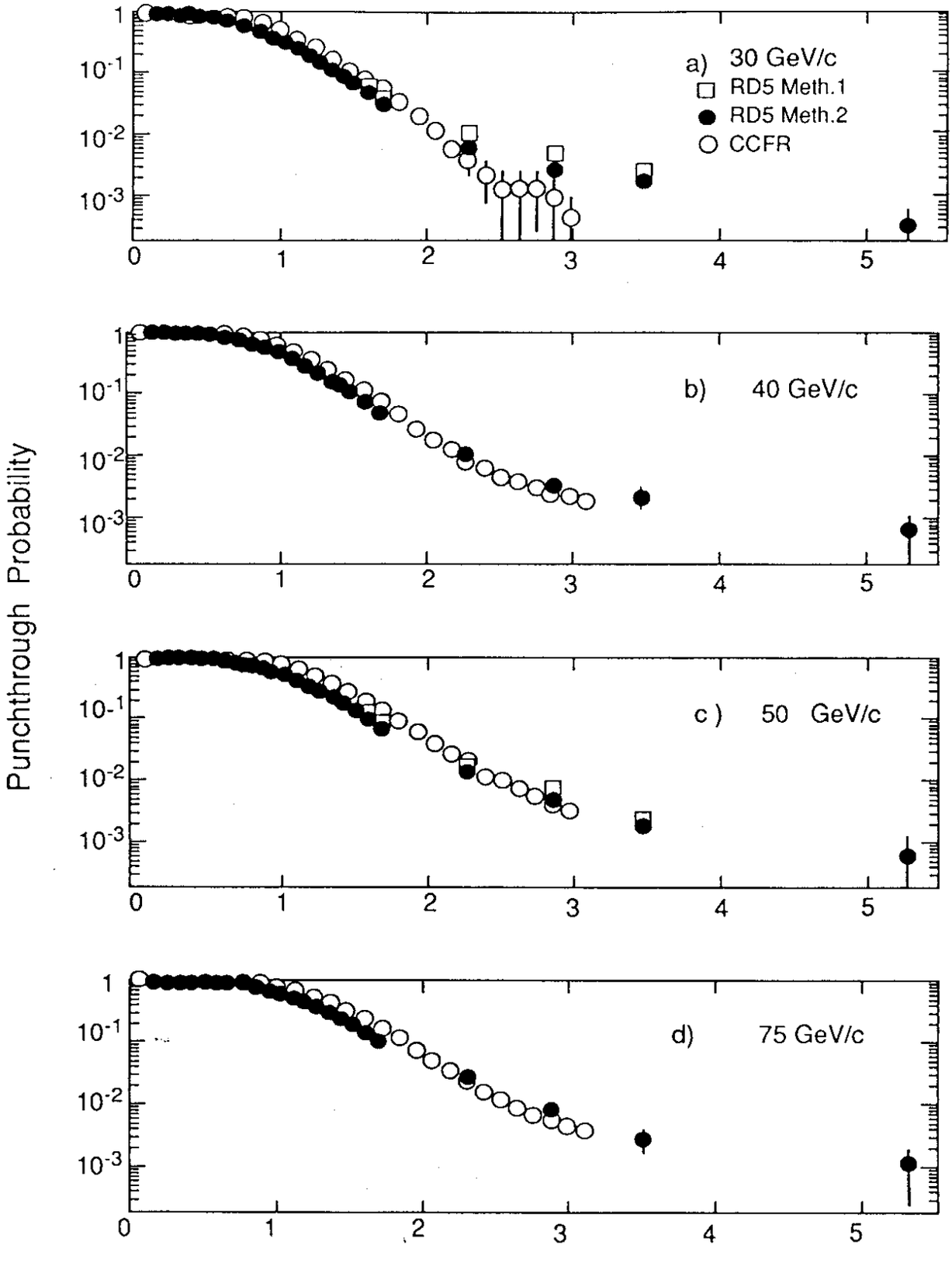
a) 30 GeV/c
RD5 Meth.1
RD5 Meth.2
CCFR
b) 40 GeV/c
c) 50 GeV/c
d) 75 GeV/c
Punchthrough Probability
m Fe Equivalent

FIG. 9